Journal of Magnetism and Magnetic Materials 655 (2026) 174312

Contents lists available at ScienceDirect

Journal of Magnetism and Magnetic Materials

journal homepage: www.elsevier.com/locate/jmmm

Eddy current testing in the quantitative assessment of the degradation state in X10CrMoVNb9–1 (P91) power engineering steel

Grzegorz Tytko [a], Karolina Piotrowska [b], Jun Tu [c], Mateusz Kopec [b,d,*]

[a] Faculty of Automatic Control, Electronics and Computer Science, Silesian University of Technology, 44-100 Gliwice, Poland
[b] Institute of Fundamental Technological Research Polish Academy of Sciences, Pawińskiego 5B, 02-106 Warsaw, Poland
[c] School of Mechanical Engineering, Hubei University of Technology, Wuhan 430068, China
[d] College of Science and Engineering, University of Derby, Markeaton Street, Derby DE22 3AW, UK

ARTICLE INFO

Keywords:
Non-destructive testing
Power engineering steels
Eddy current
Coil impedance

ABSTRACT

Ferritic–martensitic P91 steel is widely used in high-temperature power plant components due to its excellent creep resistance and mechanical stability. However, long-term service exposure and improper heat treatment can lead to progressive microstructural degradation, resulting in a reduction of mechanical properties and component lifetime. Reliable, non-destructive methods capable of detecting such microstructural changes are therefore essential for condition monitoring and life assessment. In this study, the influence of controlled heat treatment at temperatures ranging from 200 °C to 600 °C on the eddy current (EC) response of P91 steel was investigated. Eddy current measurements were performed over a range of probe operating frequencies, and changes in resistance and reactance components were quantitatively analyzed. The EC results were correlated with detailed microstructural observations, revealing a strong relationship between electromagnetic response and recovery and tempering phenomena, including dislocation density reduction, martensite lath degradation, and carbide coarsening. The findings demonstrate that eddy current testing is highly sensitive to thermally induced microstructural evolution in P91 steel and shows significant potential as a non-destructive tool for assessing thermal exposure and material degradation in power plant components.

1. Introduction

Ferritic–martensitic steels containing 9–12 wt% chromium play a critical role in modern fossil-fuel and combined-cycle power plants, where increasing operating temperatures and pressures are required to improve thermal efficiency and reduce emissions [1]. Among these materials, P91 steel (9Cr–1Mo–V–Nb) has been extensively adopted for high-temperature components such as boiler tubes, superheater and reheater pipes, headers, and steam lines. Its widespread use is primarily attributed to its favorable combination of high creep strength, good oxidation resistance, and acceptable weldability, achieved through a carefully controlled tempered martensitic microstructure [2].

The superior high-temperature performance of P91 steel is strongly dependent on the stability of its microstructure. In the normalized and tempered condition, P91 steel consists of a fine lath martensite structure with a high density of dislocations, strengthened by a dispersion of M23C6 carbides along lath and prior austenite grain boundaries, as well as fine MX precipitates within the laths [3]. This microstructure provides effective resistance to dislocation motion and creep deformation. However, exposure to elevated temperatures during service, as well as deviations from recommended heat treatment procedures, can trigger microstructural recovery and tempering processes that progressively degrade this strengthening mechanism [4].

Thermal exposure of P91 steel leads to a sequence of microstructural changes, including annihilation and rearrangement of dislocations, coarsening and redistribution of carbide precipitates, degradation of martensite lath morphology, and relaxation of internal stresses [2–5]. At sufficiently high temperatures or long exposure times, these processes may result in over-tempering, significantly reducing creep strength and increasing the susceptibility to premature failure. In practical power plant operation, such degradation may occur locally due to overheating, non-uniform temperature distribution, or long-term service beyond design conditions [6]. Early detection of these microstructural changes is therefore essential for ensuring safe operation and for implementing condition-based maintenance strategies.

Conventional techniques used to assess the microstructural condition

* Corresponding author at: Institute of Fundamental Technological Research Polish Academy of Sciences, Pawińskiego 5B, 02-106 Warsaw, Poland
E-mail addresses: grzegorz.tytko@polsl.pl (G. Tytko), kpiotrow@ippt.pan.pl (K. Piotrowska), juntu@hbut.edu.cn (J. Tu), mkopec@ippt.pan.pl (M. Kopec).

https://doi.org/10.1016/j.jmmm.2026.174312
Received 27 March 2026; Received in revised form 4 June 2026; Accepted 7 June 2026
Available online 9 June 2026

of power engineering steels include destructive metallographic examination [7], hardness measurements [8], and surface replication [9]. While these methods provide valuable insight into material state, they suffer from several limitations. Destructive testing requires material removal and is therefore not suitable for in-service inspection of critical components. Hardness testing provides only indirect information and may not be sensitive to early-stage microstructural recovery [6]. Replica techniques are restricted to surface regions and may not adequately represent bulk material degradation. These limitations have driven increasing interest in non-destructive testing (NDT) methods capable of detecting subtle microstructural changes in ferromagnetic steels.

Eddy current (EC) testing is an electromagnetic NDT technique traditionally used for detecting surface and near-surface defects, material sorting, and conductivity measurements [10–13]. In ferromagnetic materials, the EC response is governed not only by electrical conductivity but also by magnetic permeability, both of which are strongly influenced by microstructural features [14,15]. Dislocation density, precipitate size and distribution, internal stresses, and phase morphology affect electron scattering mechanisms and magnetic domain wall motion, thereby altering the resistance and reactance components of the EC signal [16]. As a result, EC testing has the potential to serve as a sensitive probe of microstructural evolution in steels subjected to thermal and mechanical degradation.

Previous studies have demonstrated the applicability of eddy current and other magnetic methods for monitoring tempering, thermal ageing, and creep damage in ferritic steels [17,18]. Mercier et al. [17] employed EC technique for evaluation of steel decarburizing. Ghanei et al. [18] proposed EC methodology for dual phase steels. Rabung et al. [19] and Kuskov et al. [20] reported application of EC for evaluation of microstructural changes induced by thermo-mechanical fatigue in ferritic and ferritic/martensitic steels. Kukla et al. [21] developed EC methodology in the non-direct measurement of martensite during plastic deformation of SS316L. Changes in EC impedance, Barkhausen noise, and magnetic hysteresis parameters have been correlated with recovery processes and mechanical property degradation [22]. Nevertheless, the majority of published work focuses on either service-exposed materials with complex degradation histories or on limited frequency ranges and single EC parameters. Systematic investigations that combine controlled heat treatments, frequency-dependent EC measurements, and detailed microstructural characterization of P91 steel remain relatively limited.

A comprehensive understanding of the relationship between specific microstructural features and EC response is essential for developing reliable diagnostic criteria applicable to industrial inspection. In particular, distinguishing between early recovery, intermediate tempering, and advanced over-tempering stages based on EC parameters would significantly enhance the usefulness of the technique for power plant applications. Such an approach requires correlating quantitative changes in EC resistance and reactance with well-defined microstructural states. Therefore, the present work aims to address this need by systematically investigating the influence of heat treatment temperature on the eddy current response and microstructure of P91 boiler steel. Samples subjected to controlled thermal exposure at temperatures between 200 °C and 600 °C were examined using eddy current testing over a range of probe operating frequencies. Changes in resistance and reactance components were quantitatively analyzed and correlated with microstructural observations obtained by metallographic examination. By linking EC parameters to specific recovery and tempering phenomena, this study seeks to evaluate the capability of eddy current testing as a non-destructive tool for assessing thermal exposure and microstructural degradation in P91 steel used in high-temperature power plant components.

2. Materials and methods

P91 samples were prepared in the form of 20mmx20mmx60mm cuboids. As received material with chemical composition presented in Table 1 was then subjected to heat treatment in air conditions at temperature of 200, 400 and 600 °C for 12 h. The temperature was selected based on operating conitions. In a power plant, water economizers typically operate at 200 °C, boiler water-wall sections and steam headers reach approximately 400 °C, and superheater tubes along with high-pressure turbine blades are subjected to extreme conditions of 600 °C.

Eddy current testing was performed using a probe incorporating a single coil with a cup core, mounted in a wooden holder (Fig. 1). This design facilitates probe handling and enables precise inspection. Impedance measurements were carried out using a Keysight E4980A precision LCR meter with an accuracy of ±0.05%. The device was connected to a measurement fixture terminated with Kelvin clips, which were attached to the probe supply leads. Measurement results were displayed on a computer screen in real time using the Keysight BenchVue software. Prior to the measurements, the instrument was calibrated using a high-precision resistor. Subsequently, a measurement mode with an extended integration time was selected to ensure outlier correction. Preliminary measurements were conducted over the probe operating frequency range from 20 Hz up to the resonance frequency, which was approximately 180 kHz. At the lowest frequencies (20–80 Hz), the measured impedance values were relatively small, resulting in a significant influence of noise and other undesirable factors. Consequently, the results were characterized by a large measurement error and pronounced oscillations. In contrast, for measurements performed at higher frequencies (above 25 kHz), the probe sensitivity was unsatisfactory, and the results obtained for different specimens were very similar. For these reasons, the final measurements were performed at 30 discrete frequency values ranging from 100 Hz to 20 kHz. Each impedance

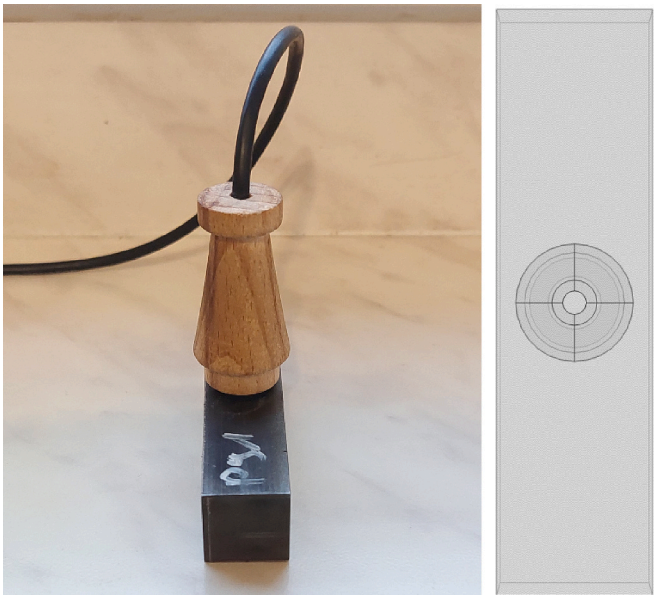

Fig. 1. General view of the eddy current probe positioned on the specimen surface (a) and schematic representation of the probe–specimen interaction (b).

Table 1
Chemical composition of X10CrMoVNb9–1 (P91) steel (wt%).

C	Mn	Cr	Mo	V	Ni	Cu	Si	S	P	Fe
0.1	0.40	8.30	0.80	0.30	0.20	0.15	0.25	0.006	<0.001	Bal.

measurement was repeated three times, and the arithmetic mean was taken as the final result. In the first step, the impedance values $Z_0 = R_0 + jX_0$ were measured at room temperature (20 °C) with the probe positioned in air. Subsequently, the probe was placed on the tested specimen and the impedance $Z = R + jX$. was measured. To reduce the error associated with the measurement method, the analysis was based on parameters describing changes in the impedance components, namely the change in resistance $\Delta R = R - R_0$ and the change in reactance $\Delta X = X - X_0$.

3. Results and discussion

In order to quantitatively evaluate the influence of heat treatment on the eddy current response of P91 steel, the relative changes in the resistance and reactance components of the probe impedance were calculated. These parameters are defined by Eqs. (1) and (2), respectively. Eq. (1) describes the relative change in the resistance component of the eddy current signal:

$$\delta R = \frac{\Delta R - \Delta R_{20^\circ C}}{\Delta R_{20^\circ C}} \cdot 100\% \quad (1)$$

where ΔR is the value of the resistance change measured for the specimen after heat treatment at temperature T, and ΔR_{20} is the corresponding change in resistance for the as-received material measured at room temperature (20 °C). The parameter δR expresses the percentage difference in resistance changes relative to the reference state. This formulation allows for direct comparison of EC resistance changes induced by thermal exposure, independent of absolute signal amplitude, which may vary with probe characteristics, lift-off conditions, or measurement setup. As a result, δR provides an effective indicator of microstructural evolution associated with recovery and tempering processes.

Eq. (2) defines the relative change in the reactance component of the eddy current signal:

$$\delta X = \frac{\Delta X - \Delta X_{20^\circ C}}{\Delta X_{20^\circ C}} \cdot 100\% \quad (2)$$

where ΔX is the value of the reactance change measured after heat treatment at temperature T, and X_{20} is the change in reactance obtained for the as-received material at room temperature. The parameter δX represents the percentage difference in reactance changes with respect to the initial microstructural state. The use of a normalized reactance change is particularly justified for ferromagnetic materials such as P91 steel, in which the reactance component is strongly influenced by magnetic permeability. Since magnetic permeability is highly sensitive to dislocation density, residual stresses, and precipitate-induced domain wall pinning, δX serves as a sensitive metric for detecting thermally induced microstructural recovery and tempering effects [23].

The change in resistance ΔR of the eddy current signal exhibits a clear and systematic dependence on heat treatment temperature for both investigated probe frequencies (Table 2, Fig. 2). For the as-received material, the highest resistance changes are observed, reflecting the high density of lattice defects characteristic of the tempered martensitic microstructure of P91 steel. At 100 Hz, the change in resistance decreases from 76.91 to 55.49 with increasing heat treatment temperature from room temperature to 600 °C, corresponding to a total reduction of approximately 28%. A similar but less pronounced trend is observed at 1 kHz, where the change in resistance decreases by about 15% over the same temperature range. The monotonic nature of these changes indicates that the EC resistance component is sensitive to thermally induced microstructural recovery processes [19].

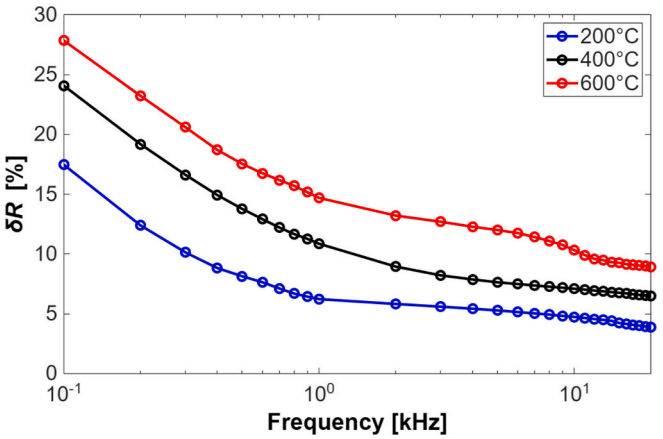

Fig. 2. Relative change in the resistance component ΔR of the eddy current signal as a function of probe operating frequency for P91 steel subjected to different heat treatment temperatures.

From a physical perspective, the reduction in resistance can be attributed primarily to changes in electrical conductivity associated with microstructural evolution [24]. Heat treatment promotes annihilation and rearrangement of dislocations, reduces internal stresses, and alters the size and distribution of carbide precipitates [25]. These processes decrease electron scattering at lattice defects and phase boundaries, leading to an increase in effective electrical conductivity and, consequently, a reduction in the resistive component of the EC signal.

The stronger relative changes observed at the lower operating frequency are related to the greater penetration depth of the eddy currents at 100 Hz, which allows for a more representative sampling of the bulk material. At higher frequencies, the EC response becomes increasingly dominated by near-surface regions, where microstructural gradients and surface conditions may partially mask bulk recovery effects.

The change in reactance ΔX shows an even more pronounced sensitivity to heat treatment temperature than resistance ΔR (Table 3, Fig. 3). At 100 Hz, the change in reactance decreases from 315.62 in the as-received condition to 258.87 after heat treatment at 600 °C, corresponding to an 18% reduction. At 1 kHz, the relative decrease reaches nearly 9%. Unlike resistance, reactance in ferromagnetic materials is strongly influenced by magnetic permeability, which is highly sensitive to microstructural features such as dislocation density, internal stress

Table 2
Maximum values of the δR coefficient of the eddy current signal measured at probe operating frequencies of 100 Hz and 1 kHz for P91 steel in the as-received condition and after heat treatment at different temperatures.

Frequency f	Sample	$\Delta R = R - R_0$ [Ω]	δR
100 Hz	20 °C	76.91 ± 0.08	–
100 Hz	200 °C	63.48 ± 0.06	17.5
100 Hz	400 °C	58.40 ± 0.06	24.1
100 Hz	600 °C	55.49 ± 0.06	27.8
1 kHz	20 °C	896.31 ± 0.90	–
1 kHz	200 °C	840.54 ± 0.84	6.2
1 kHz	400 °C	799.05 ± 0.80	10.9
1 kHz	600 °C	764.69 ± 0.76	14.7

Table 3
Maximum values of the δX coefficient of the eddy current signal measured at probe operating frequencies of 100 Hz and 1 kHz for P91 steel in the as-received condition and after heat treatment at different temperatures.

Frequency f	Sample	$\Delta X = X - X_0$ [Ω]	δX
100 Hz	20 °C	315.62 ± 0.32	–
100 Hz	200 °C	286.10 ± 0.29	9.4
100 Hz	400 °C	277.02 ± 0.28	12.2
100 Hz	600 °C	258.87 ± 0.26	18.0
1 kHz	20 °C	1499.84 ± 1.50	–
1 kHz	200 °C	1425.12 ± 1.43	5.0
1 kHz	400 °C	1403.61 ± 1.10	6.4
1 kHz	600 °C	1371.52 ± 1.37	8.6

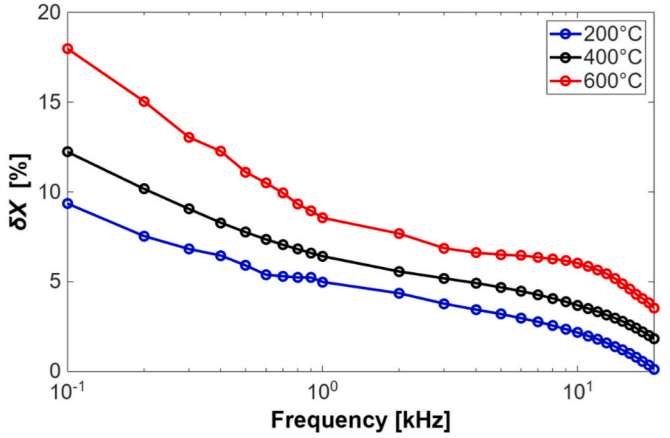

Fig. 3. Relative change in the reactance component ΔX of the eddy current signal as a function of probe operating frequency for P91 steel subjected to different heat treatment temperatures.

state, and precipitate-induced domain wall pinning. The observed decrease in reactance change with increasing heat treatment temperature therefore reflects a progressive increase in magnetic domain wall mobility [26]. At lower heat treatment temperatures (200 °C), the reduction in reactance change is modest, indicating early stages of recovery characterized by partial stress relaxation and limited dislocation rearrangement. As the temperature increases to 400 °C and 600 °C, the decrease in reactance change becomes more pronounced, consistent with advanced tempering processes involving significant lath martensite degradation and carbide coarsening. The higher sensitivity of changes in reactance compared to changes in resistance suggests that magnetic effects dominate the EC response in P91 steel during thermal exposure. This observation is particularly relevant for practical diagnostics, as magnetic parameters often respond earlier to microstructural degradation than purely electrical ones.

The eddy current response of X10CrMoVNb9–1 steel is intrinsically linked to the evolution of its tempered martensitic microstructure during thermal exposure. Each heat treatment temperature corresponds to a distinct stage of recovery and tempering, which manifests in a characteristic electromagnetic signature. In the as-received condition (Fig. 4a), P91 steel exhibits a refined lath martensite microstructure with a high density of tangled dislocations within the laths, along with a dense distribution of M23C6 carbides along lath and prior austenite grain boundaries and fine MX precipitates within the laths [27]. This microstructural state is associated with significant internal stresses and a large number of lattice defects.

From an eddy current perspective, this microstructure strongly impedes both charge carrier transport and magnetic domain wall motion. The high dislocation density and fine precipitate dispersion act as effective scattering centers for conduction electrons, resulting in the highest measured resistance values. Simultaneously, dislocations, residual stresses, and fine carbides provide numerous pinning sites for magnetic domain walls, leading to reduced magnetic permeability and elevated reactance [28]. The combination of these effects explains the pronounced EC response observed for the as-received material.

After heat treatment at 200 °C (Fig. 4b), the overall martensitic lath morphology remains largely intact; however, subtle microstructural changes are already detectable. At this temperature, thermally activated recovery processes lead primarily to partial annihilation and rearrangement of mobile dislocations, accompanied by relaxation of internal stresses. Carbide morphology and distribution remain essentially unchanged. These early recovery processes have a limited but measurable influence on the EC signal. The moderate decrease in resistance reflects a slight reduction in electron scattering due to lower dislocation density and stress fields. In contrast, the reactance exhibits a more noticeable decrease, indicating enhanced magnetic domain wall mobility resulting from stress relaxation. This observation highlights the higher sensitivity of magnetic parameters to early-stage microstructural recovery, even when conventional metallographic changes are difficult to detect.

The microstructure after heat treatment at 400 °C (Fig. 4c) shows clear evidence of advanced tempering. Martensite laths become less distinct due to progressive recovery, and a significant reduction in dislocation density is observed. At the same time, M23C6 carbides undergo noticeable coarsening and partial redistribution along boundaries, while the effectiveness of MX precipitates in stabilizing the lath structure diminishes [29]. These microstructural transformations result in pronounced changes in both EC resistance and reactance. The reduction in resistance is driven by a substantial decrease in defect-related electron scattering as the lattice becomes more ordered. However, the most significant effect is observed in the reactance component. Coarsened carbides provide fewer effective pinning points per unit volume, and the reduction of internal stresses allows magnetic domain walls to move more freely under the applied alternating magnetic field [30]. Consequently, magnetic permeability increases, leading to a marked decrease in reactance.

This stage represents a critical transition in the degradation process, where the microstructure loses much of its original strengthening architecture. The EC response at this stage clearly distinguishes the material from both the as-received and mildly recovered conditions, demonstrating the capability of the method to identify intermediate tempering.

At 600 °C (Fig. 4d), the microstructure is characterized by extensive recovery and advanced tempering. The original lath martensitic structure is severely degraded, with lath boundaries becoming blurred or partially eliminated. Dislocation density is drastically reduced, and carbide precipitates are significantly coarsened, resulting in a sparse distribution of large particles with limited strengthening capability.

This microstructural state produces the most pronounced changes in EC response. The resistance reaches its lowest values, reflecting minimal electron scattering due to the near-elimination of lattice defects and internal stresses. More importantly, the reactance decreases strongly, indicating a substantial increase in magnetic permeability. The reduced number of dislocations and coarse carbide particles offer little resistance to domain wall motion, allowing magnetic domains to respond readily to the applied electromagnetic field. From a physical standpoint, the drastic reduction in dislocation density and internal stresses allows for increased magnetic domain wall mobility, while the loss of fine carbide dispersion reduces pinning efficiency [31]. These effects dominate the EC reactance signal, explaining its higher sensitivity compared to resistance at this stage of degradation. The observed relationship between EC parameters and microstructure can be understood by considering the distinct physical mechanisms governing resistance and reactance in ferromagnetic steels. The resistance component is primarily controlled by electrical conductivity, which depends on electron scattering at lattice imperfections such as dislocations, precipitates, and stress fields. As heat treatment progresses, the systematic reduction in these defects leads to a monotonic decrease in resistance. In contrast, the reactance component is dominated by magnetic permeability, which is extremely sensitive to microstructural features that influence domain wall motion. Dislocations, fine carbides, and residual stresses act as strong pinning centers, suppressing permeability. Their gradual elimination during recovery and tempering results in disproportionately large changes in reactance, particularly at lower probe frequencies where bulk material contributes most strongly to the signal.

The frequency-dependent behavior observed in this study further supports this interpretation. Lower frequencies provide greater penetration depth, enabling the EC response to capture volumetric microstructural changes rather than surface-limited effects. This is especially relevant for power plant components, where thermal degradation typically develops over extended volumes rather than as localized surface damage. It is worth mentioning that the present results are consistent

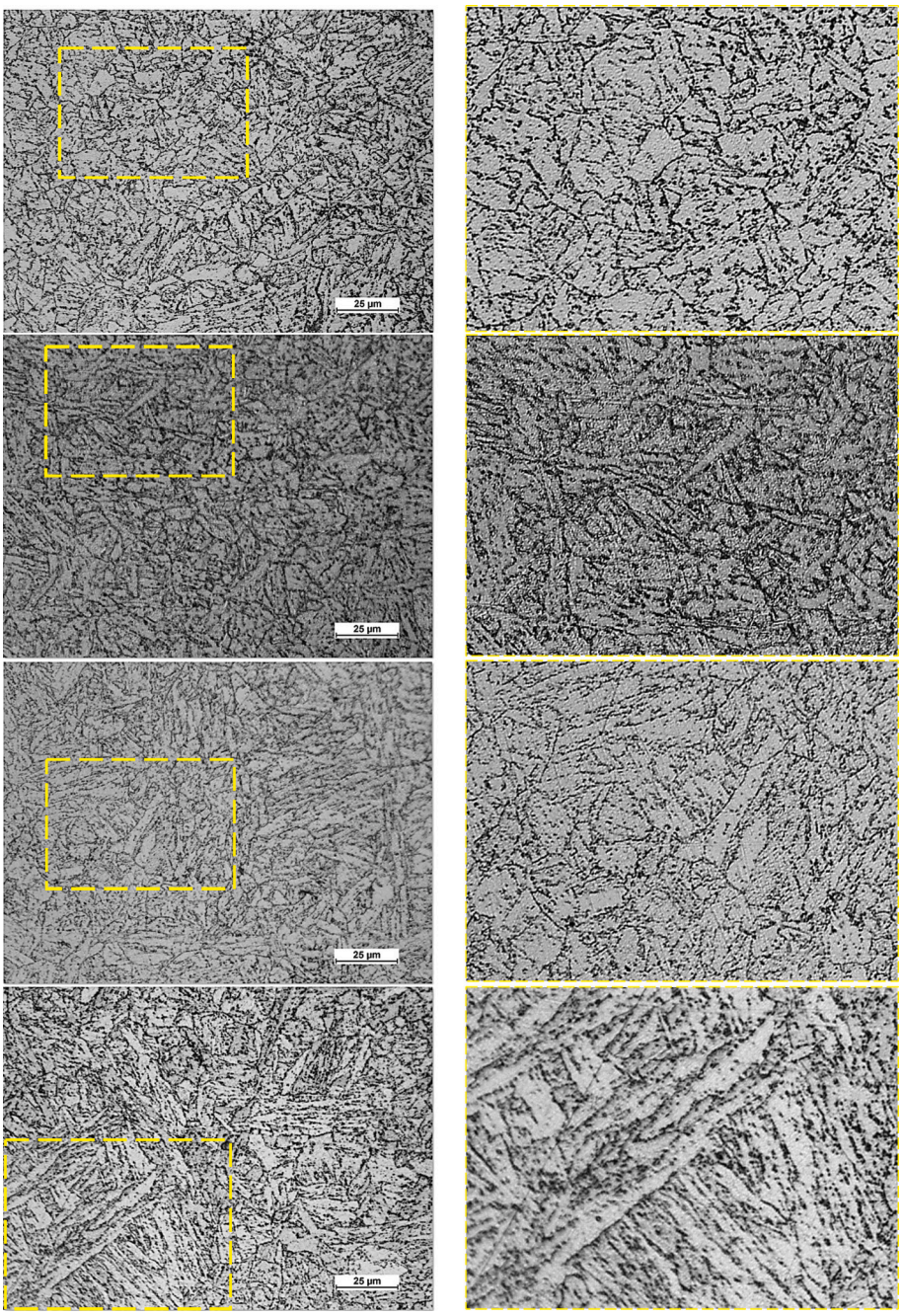

Fig. 4. Microstructure of X10CrMoVNb9–1 steel: (a) as-received condition, (b) after heat treatment at 200 °C, (c) after heat treatment at 400 °C, and (d) after heat treatment at 600 °C.

with previous studies showing that the eddy current response of steels is mainly governed by microstructure rather than residual stress when identical heat treatment conditions are applied [32]. Because microstructure is controlled by chemical composition, particularly carbon content, EC response may be indirectly influenced by composition. In ferromagnetic steels, permeability effects dominate the EC signal, leading to a decrease in impedance with increasing carbon content. Additionally, the literature reports show that increasing carbon content and hardness result in decreasing inductive reactance and increasing resistance [33]. These effects are attributed to pearlite and carbide morphology, where cementite lamellae hinder magnetic domain wall motion and increase electron scattering. As a result, harder microstructures exhibit lower reactance and higher resistance, confirming the sensitivity of eddy current testing to microstructural evolution in steels.

The results clearly demonstrate that different stages of microstructural evolution in X10CrMoVNb9–1 steel produce distinct and monotonic changes in EC parameters. Resistance changes are mainly governed by electron scattering mechanisms related to lattice defects and precipitate density, whereas reactance changes are predominantly controlled by magnetic permeability variations linked to stress state and domain wall pinning. Importantly, the EC method integrates the response from multiple microstructural features over the effective penetration depth, making it particularly suitable for assessing bulk degradation rather than localized surface effects. This is crucial for power plant components, where overheating and long-term service exposure often result in gradual, volume-averaged microstructural changes.

The higher sensitivity of reactance to thermal exposure suggests that

EC techniques focusing on magnetic parameters are especially promising for detecting early tempering, over-tempering, and creep-related degradation in ferritic–martensitic steels. As such, eddy current testing can serve as a valuable complementary technique to metallographic replication and hardness measurements in condition-based maintenance strategies for high-temperature power plant components. It should be stressed, however, that the EC response of ferromagnetic P91 steel is related not only to microstructural evolution, but also by electromagnetic factors including magnetic anisotropy, residual stresses, dislocation substructure orientation, and magnetic domain wall pinning effects [14,15,23]. In tempered martensitic steels, dislocations, carbide precipitates, and internal stress fields simultaneously affect electrical conductivity and magnetic permeability, thereby influencing both the resistive and reactive components of the EC signal [16,27,28]. Consequently, the measured impedance should be interpreted as an integrated electromagnetic response rather than a direct measurement of an individual microstructural parameter. Nevertheless, in the present study all specimens were characterized by identical geometry, surface condition, chemical composition, and probe configuration, while the only intentionally varied parameter was the heat treatment temperature. Therefore, the systematic monotonic variations observed in ΔR and ΔX can be primarily attributed to thermally induced recovery and tempering phenomena, including dislocation annihilation, stress relaxation, martensite lath degradation, and carbide coarsening [25–31]. Furthermore, although conventional high-frequency EC measurements may be dominated by near-surface geometry and topological effects due to the skin effect, the relatively low operating frequencies applied in this work (100 Hz–20 kHz) provided increased penetration depth and enhanced sensitivity to bulk material degradation. The strongest signal differentiation observed at low frequencies further supports the interpretation that the measured EC response reflects volumetric microstructural evolution rather than superficial geometrical effects [14,15,19]. Therefore, despite the inherently multiparametric nature of electromagnetic interactions in ferromagnetic steels, the obtained results demonstrate that low-frequency EC measurements can provide reliable and physically meaningful information regarding the degradation state of thermally exposed P91 steel.

Additionally, it should be mentioned, that quasi-static magnetic methods and eddy current techniques probe related but not identical electromagnetic phenomena. Quasi-static approaches are primarily sensitive to magnetization processes and are therefore often used to characterize domain-wall dynamics, magnetic anisotropy, and permeability changes associated with microstructural degradation. Eddy current measurements, in contrast, are influenced simultaneously by magnetic permeability and electrical conductivity, providing a combined electromagnetic response to microstructural evolution. Although eddy current measurements can be affected by surface geometry under certain conditions, such effects are expected to be negligible in the present study because all specimens were manufactured from the same material batch and subjected to identical machining and surface preparation procedures. Consequently, the observed differences in impedance response are attributed mainly to heat-treatment-induced microstructural changes rather than variations in surface condition. The obtained trends are consistent with reports from quasi-static magnetic techniques, which also demonstrate increased magnetic permeability and enhanced domain-wall mobility during recovery and tempering of ferritic–martensitic steels [22,23,27,30].

Nevertheless, it should be emphasized that the effectiveness of the proposed methodology was confirmed even under conditions where the heat treatment parameters differed slightly from the reference process. In the case of power engineering steels designed to withstand long-term exposure to elevated temperatures, the resulting microstructural changes are often subtle and may be difficult to detect using conventional techniques. Nevertheless, the proposed methodology demonstrated sufficient sensitivity to reliably monitor these minor variations in microstructure. Consequently, it can be regarded as a robust and reliable indicator of microstructural evolution occurring in power engineering components during service, offering valuable potential for the assessment of material degradation and remaining service life.

4. Conclusions

Based on the experimental results and their correlation with microstructural observations, the following conclusions can be drawn:

1. Controlled heat treatment of P91 steel in the temperature range of 200–600 °C produces systematic and monotonic changes in both resistance and reactance components of the eddy current signal.
2. The resistance component decreases with increasing heat treatment temperature due to reduced electron scattering associated with dislocation recovery, stress relaxation, and carbide coarsening.
3. The reactance component exhibits higher sensitivity to thermal exposure than resistance, reflecting strong changes in magnetic permeability caused by increased domain wall mobility and reduced pinning.
4. Eddy current measurements performed at lower probe frequencies show greater sensitivity to bulk microstructural degradation, highlighting the importance of frequency selection in practical applications.
5. The observed EC signal variations correlate directly with microstructural evolution, from early recovery at 200 °C to advanced tempering and martensite lath degradation at 600 °C.
6. Eddy current testing demonstrates strong potential as a non-destructive technique for assessing thermal exposure and degradation state of ferritic–martensitic P91 steel in high-temperature power plant components.

Further work is needed to achieve greater probe sensitivity, enabling the detection of even slight structural changes. Several ideas that could significantly improve the effectiveness of eddy current inspections are considered. In the first step, the sensitivity of the measurement system will be increased by designing a probe consisting of several coils operating in a transmitter-receiver configuration. Next, a magnetic field sensor will be used to assist the probe's operation. This solution will enable the measurement and analysis not only of impedance components but also of magnetic field strength. In the final step, the prepared measurement system will be tested using pulsed eddy current (PEC). Analysis of the obtained results will be used to select the most effective probe design, which will be applied to perform measurements at high temperatures using a furnace connected to an LCR analyzer.

CRediT authorship contribution statement

Grzegorz Tytko: Writing – original draft, Visualization, Validation, Supervision, Software, Methodology, Investigation, Formal analysis, Data curation, Conceptualization. **Karolina Piotrowska:** Methodology, Investigation. **Jun Tu:** Validation, Methodology, Formal analysis. **Mateusz Kopec:** Writing – review & editing, Writing – original draft, Visualization, Validation, Supervision, Software, Resources, Project administration, Methodology, Investigation, Funding acquisition, Formal analysis, Data curation, Conceptualization.

Declaration of competing interest

The authors declare that they have no known competing financial interests or personal relationships that could have appeared to influence the work reported in this paper.

Acknowledgements

The authors would like to express their gratitude to Mr. M. Wyszkowski and Prof. D. Kukla for their kind help during the experimental

part of this work.

Data availability

Data will be made available on request.

References

[1] M. Kopec, A. Brodecki, D. Kukla, et al., Suitability of DIC and ESPI optical methods for monitoring fatigue damage development in X10CrMoVNb9-1 power engineering steel, Arch. Civ. Mech. Eng. 21 (2021) 167, https://doi.org/10.1007/s43452-021-00316-1.

[2] M. Kopec, D. Kukla, A. Brodecki, Z.L. Kowalewski, Effect of high temperature exposure on the fatigue damage development of X10CrMoVNb9–1 steel for power plant pipes, International Journal of Pressure Vessels and Piping, ISSN: 0308–0161, DOI: 10.1016/j.ijpvp.2020.104282, Vol.189, pp.104282–1-16, 2021.

[3] R. Bonetti, N.C. Neate, A. Morris, P.H. Shipway, W. Sun, Microstructure evolution and deformation mechanisms of service-exposed P91 steel via interrupted uniaxial creep tests at 660°C, J. Mater. Res. Technol. 33 (2024) 3529–3549, https://doi.org/10.1016/j.jmrt.2024.10.045.

[4] H. Zhou, J. Li, J. Liu, et al., Significant reduction in creep life of P91 steam pipe elbow caused by an aberrant microstructure after short-term service, Sci. Rep. 14 (2024) 5216, https://doi.org/10.1038/s41598-024-55557-w.

[5] Facai Ren, Jinsha Xu, Zhiqiu Tu, Jun Si, Microstructure analysis of P91 heat resistant steel in service for 3 years, J. Phys.: Conf. Ser. 1885 (2021) 052037, https://doi.org/10.1088/1742-6596/1885/5/052037.

[6] Xiaoxiang Sun, Chang Che, Gong Qian, Xue Wang, Microstructure, hardness and creep properties for P91 steel after long-term service in a ultra-supercritical power plant, Int. J. Press. Vessel. Piping, Volume 212, Part A (2024) 105330, https://doi.org/10.1016/j.ijpvp.2024.105330.

[7] K. Majchrowicz, B. Romelczyk-Baishya, M. Wieczorek-Czarnocka, S. Marciniak, M. Mras, D. Kukla, M. Kopec, Z. Pakieła, Assessment of 10CrMo9-10 power engineering steel degradation state by using small punch test, Materials 18 (2025) 4133, https://doi.org/10.3390/ma18174133.

[8] S.H. Hashemi, D. Mohammadyani, Characterisation of weldment hardness, impact energy and microstructure in API X65 steel, Int. J. Press. Vessel. Pip. 98 (2012) 8–15, https://doi.org/10.1016/j.ijpvp.2012.05.011.

[9] D. Bricín, Z. Špirit, J. Brom, Collection of Replicas to Evaluate the Structural Condition of Steel after Thermal Ageing, Key Eng. Mater. (Volume 1034) (2026) 113–118, https://doi.org/10.4028/p-ZvjOu0.

[10] Y. Du, Z. Zhang, W. Yin, et al., Sloping-invariance for nonferrous metallic slabs at multiple frequencies by eddy current sensors, IEEE Access 9 (2021) 59949–59956.

[11] P. Huang, J. Long, J. Jia, K. Liu, X. Yu, L. Xu, Y. Xie, Measurement of conductivity and diameter of metallic rods using eddy current testing, Measurement 221 (2023) 113496.

[12] G. Tytko, Eddy current testing of conductive coatings using a pot-core sensor, Sensors 23 (2) (2023) 1042.

[13] T.D. Ngo, T.H. Trieu, N. Kasai, J. Lee, M. Le, Pot-Core hall probe with multivariate empirical mode decomposition based on spatial filtering for quantitative pulsed eddy current measurement of subsurface corrosion, Measurement 266 (2026) 120517.

[14] Z. Deng, Z. Yu, Z. Yuan, X. Song, Y. Kang, Mechanism of magnetic permeability perturbation in magnetizing-based eddy current nondestructive testing, Sensors 22 (7) (2022) 2503.

[15] P. Huang, J. Zhao, Z. Li, H. Pu, Y. Ding, L. Xu, Y. Xie, Decoupling conductivity and permeability using sweep-frequency eddy current method, IEEE Trans. Instrum. Meas. 72 (2023) 1–11.

[16] I.M. Oliveira Anício Costa, M. Batková, I. Batko, A. Benabou, C. Mesplont, J.-B. Vogt, The influence of microstructure on the electromagnetic behavior of carbon steel wires, Crystals 12 (2022) 576, https://doi.org/10.3390/cryst12050576.

[17] D. Mercier, J. Lesage, X. Decoopman, D. Chicot, Eddy currents and hardness testing for evaluation of steel decarburizing, NDT & E International 39 (8) (2006) 652–660, https://doi.org/10.1016/j.ndteint.2006.04.005.

[18] Sadegh Ghanei, Mehrdad Kashefi, Mohammad Mazinani, Eddy current nondestructive evaluation of dual phase steel, Mater. Des. 50 (2013) 491–496, https://doi.org/10.1016/j.matdes.2013.03.040.

[19] M. Rabung, K. Schmitz, O. Sanliturk, P. Lehner, B. Blinn, T. Beck, Non-destructive evaluation of microstructural changes induced by thermo-mechanical fatigue in ferritic and ferritic/martensitic steels, Appl. Sci. 15 (2025) 4969, https://doi.org/10.3390/app15094969.

[20] K.V. Kuskov, R.A. Sokolov, K.R. Muratov, Application of the Eddy current method of control for indication of fatigue changes in austenitic steels with martensite formation, Russ. J. Nondestruct. Test. 61 (2025) 804–810, https://doi.org/10.1134/S1061830925700202.

[21] Dominik Kukla, Adam Kondej, Sylwester Jończyk, Piotr Lasota, Jakub Tabin, Daniela Schob, Robert Roszak, Jakub Kawałko, Andrzej Zagórski, Mateusz Kopec, Eddy current methodology in the non-direct measurement of martensite during plastic deformation of SS316L, open Engineering 15 (1) (2025) 20250118, https://doi.org/10.1515/eng-2025-0118.

[22] P. Vourna, P.P. Falara, A. Ktena, E.V. Hristoforou, N.D. Papadopoulos, Magnetic Barkhausen noise sensor: a comprehensive review of recent advances in non-destructive testing and material characterization, Sensors 26 (2026) 258, https://doi.org/10.3390/s26010258.

[23] H. Sheng, P. Wang, Y. Yang, C. Tang, Stress and microstructures characterization based on magnetic incremental permeability and magnetic Barkhausen noise techniques, Materials (Basel). 17 (11) (2024) 2657, https://doi.org/10.3390/ma17112657.

[24] Lin Chen, Meigui Ou, Yu Liang, Yilong Liang, Effects of processing paths on microstructure evolution and properties of high-strength and high-conductivity Al-Mg-Si alloys, Materials Science and Engineering: A 941 (2025) 148606, https://doi.org/10.1016/j.msea.2025.148606.

[25] Sylvain Dépinoy, Microstructural evolution of a 2.25Cr - 1 Mo steel during austenitization and temper :austenite grain growth, carbide precipitation sequence and effects on mechanical properties, Materials. Ecole Nationale Supérieure des Mines de Paris (2015) (English. NNT : 2015ENMP0049).

[26] Xiangyi Hu, Zhensheng Fu, Jianhua Zhang, Yunfang Long, The effect of heat treatment on microstructure and magnetic domain related to magnetization characteristics in Q345R steels, Journal of Magnetism and Magnetic Materials 555 (2022) 169377, https://doi.org/10.1016/j.jmmm.2022.169377.

[27] Y. Li, C. Sun, K. Liu, T. Xu, B. He, Magnetic evaluation of heat-resistant martensitic steel subjected to microstructure degradation, Materials 15 (2022) 4865, https://doi.org/10.3390/ma15144865.

[28] S. Ghanei, A. Saheb Alam, M. Kashefi, M. Mazinani, Nondestructive characterization of microstructure and mechanical properties of intercritically annealed dual-phase steel by magnetic Barkhausen noise technique, Materials Science and Engineering: A, 607, 2014, ages 253-260, Doi: https://doi.org/10.1016/j.msea.2014.04.026.

[29] A. Grajcar, M. Morawiec, J.A. Jimenez, C. Garcia-Mateo, Dilatometric and microstructural study of martensite tempering in 4% Mn steel, Materials 13 (2020) 4442, https://doi.org/10.3390/ma13194442.

[30] K.S. Ryu, S.H. Nahm, J.S. Park, K.M. Yu, Y.B. Kim, D. Son, A new non-destructive method for estimating the remanent life of a turbine rotor steel by reversible magnetic permeability, J. Magn. Magn. Mater. 251 (2002) 196–201.

[31] Suvi Santa-aho, Mari Honkanen, Sami Kaappa, Lucio Azzari, Andrey Saren, Kari Ullakko, Lasse Laurson, Minnamari Vippola, Multi-instrumental approach to domain walls and their movement in ferromagnetic steels – origin of Barkhausen noise studied by microscopy techniques, Mater. Des. 234 (2023) 112308, https://doi.org/10.1016/j.matdes.2023.112308.

[32] Meisam Sheikh Amiri, Mehrdad Kashefi, application of eddy current nondestructive method for determination of surface carbon content in carburized steels, NDT & E International 42 (7) (2009) 618–621, https://doi.org/10.1016/j.ndteint.2009.04.008.

[33] A. Isadora, M.O.A. Costa, et al., IOP Conf. Ser.: Mater. Sci. Eng. 859 (2020) 1–7, https://doi.org/10.1088/1757-899X/859/1/012005, 012005.